INTERNATIONAL JOURNAL OF PRECISION ENGINEERING AND MANUFACTURING Vol. 16, No. 7, pp. 1501-1508 JUNE 2015 / 1501
DOI: 10.1007/s12541-015-0199-6 ISSN 2234-7593 (Print) / ISSN 2005-4602 (Online)

# Construction and Validation of Optimal Design Framework for Marine Systems based on Neuro-Response Surface Method

**Jae-Chul Lee[1], Sung-Chul Shin[1,#], and Soo-Young Kim[1]**

1 Department of Naval Architecture and Ocean Engineering, Pusan National University, 2, Busandaehak-ro 63beon-gil, Geumjeong-gu, Busan, 609-717, South Korea
# Corresponding Author / E-mail: scshin@pusan.ac.kr, TEL: +82-51-510-2525, FAX: +82-51-510-8836

KEYWORDS: Optimal design framework, Neuro-response surface method (NRSM), Back-propagation neural network (BPN), Non-dominated sorting genetic algorithm-II (NSGA-II), Substructure of floating offshore wind turbine

*The geometry of systems including the marine engineering problems needs to be optimized in the initial design stage. However, the performance analysis using commercial code is generally time consuming. To solve this problem, many engineers perform the optimization process using the response surface method (RSM) to predict the system performance, but RSM presents some prediction errors for nonlinear systems. The major objective of this research is to establish an optimal design framework for marine systems. The framework is composed of three parts: definition of geometry, generation of response surface, and optimization process. To reduce the time for performance analysis and minimize the prediction errors, the response surface is generated using the back-propagation neural network (BPN) which is considered as neuro-response surface method (NRSM). The optimization process is done for the generated response surface by non-dominated sorting genetic algorithm-II (NSGA-II).A nonlinear mathematical function problem is used to compare the accuracy of response surface generated by RSM and NRSM. Through case study of substructure of floating offshore wind turbine considering hydrodynamic performance, we have confirmed the proposed framework applicability for marine system optimization. In the future, we will try to apply the optimization problem for marine systems using the constructed framework.*

Manuscript received: July 29, 2014 / Revised: February 3, 2015 / Accepted: April 27, 2015

## 1. Introduction

The system performance is severely affected by the geometry. For this reason, determining an optimal geometry is one of the challenging problems in the initial design stage. In recent years, system optimization based on the performance using the commercial code is a method that was employed for engineering design problem.[1,2]

The essence of optimization design process is the performance analysis according to the geometry changes. Generally, the performance analysis of the complex engineering system is time consuming. To reduce the performance calculation time, many researchers use the response surface method (RSM) to predict the performance (Fig. 1),[3-5] but the method produces some errors in highly nonlinear problems.[6-8]

Naval architecture and ocean engineering (NAOE) optimization problems based on performance involve highly nonlinear elements, such as hull forms, super-structures, propeller, and offshore structure.

Up to now, many relevant papers about optimization based on system performance have been published. To predict the system performance, Shin[9] employed the neuro-fuzzy algorithm to predict the wake distribution, Xu[10] predicted the maritime safety using the artificial neural network (ANN), and Lee[11] tried the prediction for added resistance in waves using the genetic programming (GP). To optimize the shape based on performance, Lee and Choi[12] tried to optimize the hull form using the form parametric design method, and Kim[13] developed a framework to optimize the stern form based on CFD. In the shape optimization research, CFD calculation was just a means of checking performance of a design process. To search widely for the optimum design and reduce the performance analysis time, we need to construct an optimal design framework that includes performance prediction and optimization process.

The main objective of this research is to establish an optimal design framework for the marine system while considering its performance. For this purpose, we propose an optimization framework based on two principal phases:

($1^{st}$ Phase)

To predict the system performance, generate the response surface

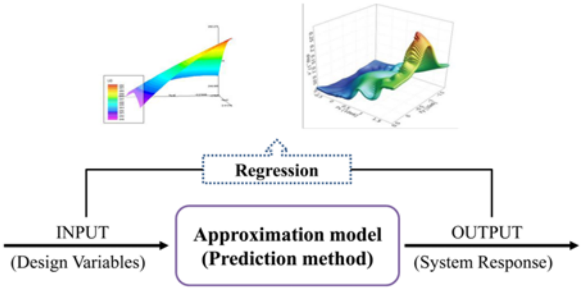


Fig. 1 Response surface method (RSM)

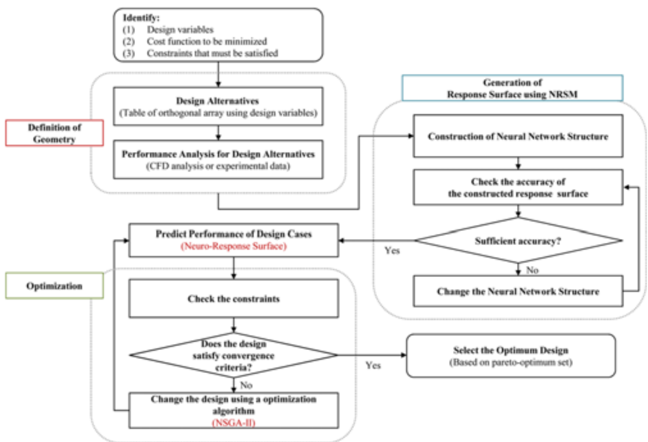


Fig. 2 Optimal design framework based on NRSM

using the artificial neural network that is considered as neuro-response surface method (NRSM) in the proposed framework.

($2^{nd}$ Phase)

Optimize the shape in the generated response surface.

The framework was validated through the range of design variable optimization problem of a 5MW TLP-type wind-turbine considering hydrodynamic performance.

## 2. Framework for Optimum Design based on NRSM

The optimal design framework includes shape representation, performance prediction and optimization. Fig. 2 illustrates the framework which is composed of three parts:

($1^{st}$ process: Definition of the geometry)

The framework defines the shape of the structure by parameterization. An orthogonal array table[14] is used for the systematic generation of design alternatives, and the performance analysis results of the alternative designs are used to generate the response surface.

($2^{nd}$ process: Generation of response surface using NRSM)

The multi-layer perceptron (MLP) was used to generate the response surface. It has three layers: an input layer, hidden layer, and output layer. The back-propagation algorithm[15] was used to train the neural network. The response surface is very important because the optimization process is done on it. In order to construct the appropriate response surface, the best structure and the best number of learning cycles for the neural network was prepared and the prediction accuracy of the generated response surface was confirmed. To check the interaction between the variables and the response, the generated design alternatives ($1^{st}$ process) are divided into 2 sets:

- Training data: used to generate the response surface.
- Test data: used to check the prediction accuracy.

After generating the response surface, the performance of various design alternatives can be predicted easily and quickly.

($3^{rd}$ process: Optimization)

The optimization process is done for the generated response surface. The NSGA-II[16] is used as a multi-objective optimization algorithm.

Finally, the optimum structural design can be selected using the pareto-optimum set which results from the proposed framework. The framework is constructed using MATLAB code.

### 2.1 Need for the generating response surface using NRSM

RSM is used to define the relationship between the response and design variables. However, the major disadvantage of RSM is to fit the data linear ($1^{st}$ order) or nonlinear ($2^{nd}$ order) polynomial function. Many engineering problems, however, are not included by polynomial function. On the other hand, ANN has an advantage for the definition of the nonlinear relationship between response and design variables, and this method is useful for the multi-inputs and multi-outputs relationship modeling. ANN defines the relationship by three types of parameter:[17]

- The interconnection node between each layer of neurons
- The learning process for updating the corresponding synaptic weights of the interconnections
- To determine an output, the signal transfer function that transforms neuron's internal activation

To generate the suitable response surface for marine system problem, we analyzed the response surface generated by polynomial model and NRSM. A nonlinear mathematical function was used for this purpose (Eq. (1)). 25 sets of data were generated (Table 1).

$$f(x_1,x_2) = 20+x_1^2+x_2^2-10\times(\cos(2\pi x_1)+\cos(2\pi x_2)) \qquad (1)$$

s.t. $1 \le x_i \le 5$ , $i = 1,2$ ; $x_i$ is a real number

Case 5, 10, 15, 20, and 25 (Table 1) were used to check the accuracy of the response surface generated by polynomial regression and NRSM.

We used a polynomial model to generate the response surface. The design variables are used until the $4^{th}$ degree (Eq. (2)). Fig. 3 shows the response surface generated using the polynomial regression. $x_1$ and $x_2$ are the design variables and $F(x_1, x_2)$ is the calculation result.

$$\begin{aligned} F(x_1,x_2) = {} & 0.6562+(0.08951*x_1)+(0.05897*x_2)+ \\ & (0.02137*x_1^2)+(-3.11E^{-17}*x_1*x_2)+ \\ & (0.0901*x_2^2)+(-4.46E^{-17}*x_1^3)+ \\ & (1.08E^{-17}*x_1^2*x_2)+(-6.36E^{-17}*x_1*x_2^2)+ \\ & (-8.75E^{-17}*x_2^3)+(-1.04E^{-17}*x_1^2*x_2^2)+ \\ & (-1.53E^{-17}*x_1^3*x_2)+(1.04E^{-17}*x_1^2*x_2^2)+ \\ & (-2.97E^{-17}*x_1*x_2^3)+(0.05306*x_2^4) \end{aligned} \qquad (2)$$

Table 1 Results of performance analysis

| Case | Design variables | | Calculation |
|---|---|---|---|
| | $x_1$ | $x_2$ | $f(x_1, x_2)$ |
| 1 | 1.000 | 1.000 | 2.000 |
| 2 | 1.000 | 2.000 | 5.000 |
| 3 | 1.000 | 3.000 | 10.000 |
| 4 | 1.000 | 4.000 | 17.000 |
| 5 | 1.000 | 5.000 | 26.000 |
| 6 | 2.000 | 1.000 | 5.000 |
| 7 | 2.000 | 2.000 | 8.000 |
| 8 | 2.000 | 3.000 | 13.000 |
| 9 | 2.000 | 4.000 | 20.000 |
| 10 | 2.000 | 5.000 | 29.000 |
| 11 | 3.000 | 1.000 | 10.000 |
| 12 | 3.000 | 2.000 | 13.000 |
| 13 | 3.000 | 3.000 | 18.000 |
| 14 | 3.000 | 4.000 | 25.000 |
| 15 | 3.000 | 5.000 | 34.000 |
| 16 | 4.000 | 1.000 | 17.000 |
| 17 | 4.000 | 2.000 | 20.000 |
| 18 | 4.000 | 3.000 | 25.000 |
| 19 | 4.000 | 4.000 | 32.000 |
| 20 | 4.000 | 5.000 | 41.000 |
| 21 | 5.000 | 1.000 | 26.000 |
| 22 | 5.000 | 2.000 | 29.000 |
| 23 | 5.000 | 3.000 | 34.000 |
| 24 | 5.000 | 4.000 | 41.000 |
| 25 | 5.000 | 5.000 | 50.000 |

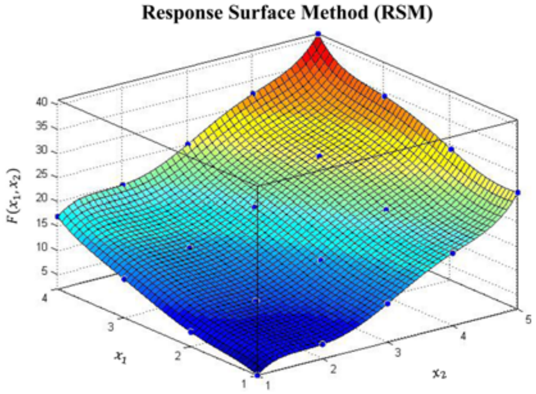


Fig. 3 Nonlinear polynomial response surface

Fig. 4 shows the response surface generated using the NRSM. The neural network structure (2-3-1) is illustrated in Fig. 5.

Table 2 shows the prediction errors of each method. The "desired values" are the calculation results, and the "prediction values" are the output of the polynomial model and NRSM. The error is defined by the below Eq. (3):

$$Error = (Desired\ value - Prediction\ value)/Desired\ value \quad (3)$$

The prediction values given by NRSM are more accurate than the polynomial model. Therefore, NRSM is considered a more suitable method to generate the response surface for high nonlinearity problems

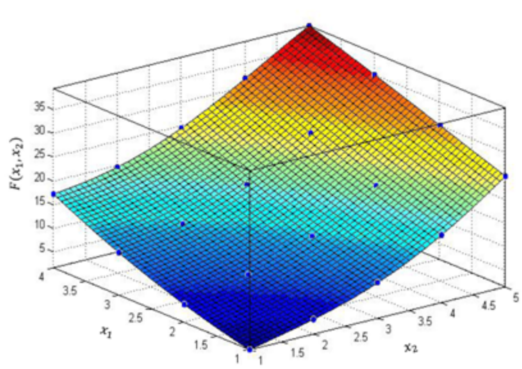


Fig. 4 Neuro-Response Surface Method (NRSM)

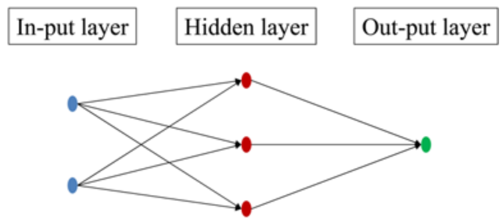


Fig. 5 Neural network structure

Table 2 Results of test data

| Case | Calculation results | | | Error | |
|---|---|---|---|---|---|
| | Desired | Prediction (Polynomial) | Prediction (NRSM) | Polynomial | NRSM |
| 5 | 26.000 | 23.910 | 25.032 | 0.080 | 0.037 |
| 10 | 29.000 | 25.272 | 27.166 | 0.129 | 0.063 |
| 15 | 34.000 | 26.699 | 31.610 | 0.215 | 0.070 |
| 20 | 41.000 | 28.190 | 37.714 | 0.312 | 0.080 |
| 25 | 50.000 | 29.745 | 43.540 | 0.405 | 0.129 |

than polynomial model. The optimal design framework is proposed using this method.

## 3. Case Study

To confirm the usability of the proposed framework, a 5MW TLP-type wind-turbine is used for a case study while considering hydrodynamic performance (nacelle acceleration and line tension). The accuracy of the framework results has been analysed using commercial software (AQWA).

### 3.1 Formulation of optimization problem

The equation below shows the formulation process of the optimization problem for a 5MW TLP-type wind turbine substructure while considering nacelle acceleration, and line tension (Eqs. (4)-(5)).

Find $x_i$

$x_i$ = Design Variables ($i = 1, 2, 3$)

to minimize

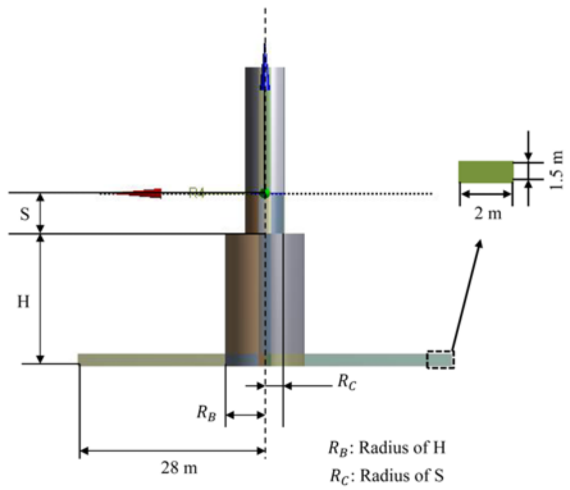


Fig. 6 Design model

$$F(x) = (W_1 \times f_1) + (W_2 \times f_2) \tag{4}$$

where,

$f_1(x)$ = Nacelle Acceleration (g)

$f_2(x)$ = Line Tension (N)

$W_i$ = Weighting factor ($i = 1, 2$)

subject to

$$\min x_i \leq x_i \leq \max x_i \tag{5}$$

$i = 1, 2, 3$ ($i$ = number of design variables)

Three design variables are considered: S (the submerged depth for a column), H (the height of the cylinder) and $R_B$ (the cylinder radius). Fig. 6 shows the design model including the design variables. At this time, S is set as the depth at 20% or 40% of the total area.

### 3.2 Environmental conditions

The Gulf of Mexico was considered for the environmental conditions. Table 3 shows the environmental conditions.

### 3.3 Definition of geometry

The proposed framework defines the shape of the structure by parameterization. The generated geometries are used to generate the response surface. 18 sets of different design alternatives are generated using an orthogonal array table ($L_{18}(2^1 \times 3^2)$) as shown in Table 4. Table 5 shows the results of the performance analysis for nacelle acceleration and line tension using the AQWA (commercial software).

After performance calculation of the generated design cases, the response surface was generated using NRSM. Then, we predicted the performance of the design cases in a continuous response surface that was not directly computed. We used 15 sets of data (Table 9) to generate the response surface and 3 sets of data (Table 6) to check its accuracy.

### 3.4 Generation of response surface using NRSM

The number of hidden layers was changed from 1 to 10. Using six hidden layers gave a better result. Therefore, the final structure and the number of learning cycles are 3-6-2 and 20000, respectively. Figs. 7 and 8 show the structure and the error convergence in the learning process of the neural network. The error convergence (0.005) occurs at approximately 16500 iterations.

The error is defined in Eqs. (6) and (7). The error value between the output of the network ($d_j$) and the actual value ($y_i$) is used. $L$ is the number of output neurons.

Table 3 Environment conditions

| Wave | | | | |
|---|---|---|---|---|
| Spectrum | Significant wave height | Period | Peak period | Gamma ($\gamma$) |
| Jonswap | 7.3 (m) | 16 (s) | 0.411 (Hz) | 2 |
| Wind | | | | |
| Spectrum | Reference height | Wind speed | Direction | |
| API | 10 (m) | 23.9 (m/s) | 0° | |

Table 4 Design alternatives

| Case | Design variables | | | |
|---|---|---|---|---|
| | S (m) | $R_B$ (m) | H (m) | Remark |
| 1 | 6 | 6 | 20 | - |
| 2 | 15 | 6 | 20 | - |
| 3 | 6 | 6 | 25 | - |
| 4 | 15 | 6 | 25 | - |
| 5 | 6 | 6 | 30 | - |
| 6 | 15 | 6 | 30 | - |
| 7 | 6 | 8 | 20 | - |
| 8 | 15 | 8 | 20 | - |
| 9 | 6 | 8 | 25 | Base design |
| 10 | 15 | 8 | 25 | - |
| 11 | 6 | 8 | 30 | - |
| 12 | 15 | 8 | 30 | - |
| 13 | 6 | 10 | 20 | - |
| 14 | 15 | 10 | 20 | - |
| 15 | 6 | 10 | 25 | - |
| 16 | 15 | 10 | 25 | - |
| 17 | 6 | 10 | 30 | - |
| 18 | 15 | 10 | 30 | - |

Table 5 Results of performance analysis

| Case | Nacelle acceleration (g) | Line tension (N) |
|---|---|---|
| 1 | 0.345 | 1862740.000 |
| 2 | 0.185 | 2295493.500 |
| 3 | 0.219 | 2573576.250 |
| 4 | 0.181 | 2653605.000 |
| 5 | 0.206 | 2876034.250 |
| 6 | 0.169 | 2977680.750 |
| 7 | 0.255 | 2745077.000 |
| 8 | 0.203 | 3242407.250 |
| 9 | 0.237 | 3153885.750 |
| 10 | 0.190 | 3817764.750 |
| 11 | 0.218 | 3825181.000 |
| 12 | 0.177 | 4503894.000 |
| 13 | 0.271 | 3940402.000 |
| 14 | 0.212 | 4247608.000 |
| 15 | 0.249 | 3580220.750 |
| 16 | 0.197 | 3775073.000 |
| 17 | 0.225 | 6142682.000 |
| 18 | 0.183 | 6036633.000 |

Table 6 Training data

| Case | S (m) | $R_B$ (m) | H (m) | Nacelle acceleration (g) | Line tension (N) |
|---|---|---|---|---|---|
| 1 | 6 | 6 | 20 | 0.345 | 1862740.000 |
| 2 | 15 | 6 | 20 | 0.185 | 2295493.500 |
| 3 | 6 | 6 | 25 | 0.219 | 2573576.250 |
| 4 | 15 | 6 | 25 | 0.181 | 2653605.000 |
| 6 | 15 | 6 | 30 | 0.169 | 2977680.750 |
| 7 | 6 | 8 | 20 | 0.255 | 2745077.000 |
| 8 | 15 | 8 | 20 | 0.203 | 3242407.250 |
| 9 | 6 | 8 | 25 | 0.237 | 3153885.750 |
| 11 | 6 | 8 | 30 | 0.218 | 3825181.000 |
| 12 | 15 | 8 | 30 | 0.177 | 4503894.000 |
| 13 | 6 | 10 | 20 | 0.271 | 3940402.000 |
| 14 | 15 | 10 | 20 | 0.212 | 4247608.000 |
| 16 | 15 | 10 | 25 | 0.197 | 3775073.000 |
| 17 | 6 | 10 | 30 | 0.225 | 6142682.000 |
| 18 | 15 | 10 | 30 | 0.183 | 6036633.000 |

Table 7 Test data

| Case | S (m) | $R_B$ (m) | H (m) | Nacelle acceleration (g) | Line tension (N) |
|---|---|---|---|---|---|
| 5 | 6 | 6 | 30 | 0.206 | 2876034.250 |
| 10 | 15 | 8 | 25 | 0.190 | 3817764.750 |
| 15 | 6 | 10 | 25 | 0.249 | 3580220.750 |

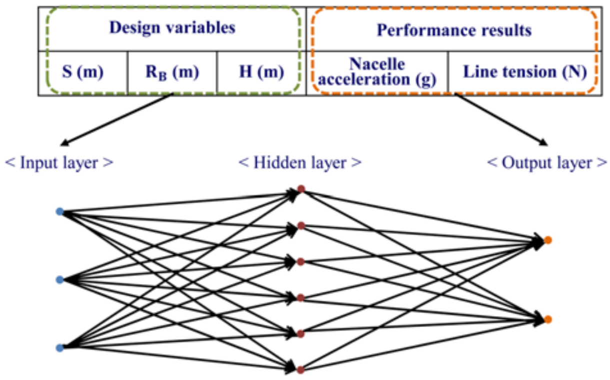


Fig. 7 Structure of BPN

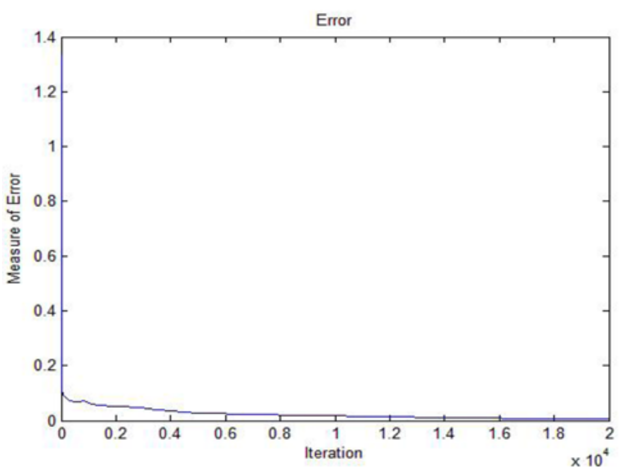


Fig. 8 Measure of error

Table 8 Analysis results for training data set

| Case | Desired values (AQWA) | | Prediction values (NRSM) | |
|---|---|---|---|---|
| | Nacelle acceleration (g) | Line tension (N) | Nacelle acceleration (g) | Line tension (N) |
| 1 | 0.345 | 1862740.000 | 0.339 | 1845620.232 |
| 2 | 0.185 | 2295493.500 | 0.186 | 2213695.244 |
| 3 | 0.219 | 2573576.250 | 0.222 | 2367773.156 |
| 4 | 0.181 | 2653605.000 | 0.180 | 2453371.996 |
| 6 | 0.169 | 2977680.750 | 0.171 | 2693048.748 |
| 7 | 0.255 | 2745077.000 | 0.256 | 2675928.980 |
| 8 | 0.203 | 3242407.250 | 0.203 | 3249441.208 |
| 9 | 0.237 | 3153885.750 | 0.234 | 3172402.252 |
| 11 | 0.218 | 3825181.000 | 0.214 | 3985591.232 |
| 12 | 0.177 | 4503894.000 | 0.175 | 4516304.040 |
| 13 | 0.271 | 3940402.000 | 0.266 | 3891432.508 |
| 14 | 0.212 | 4247608.000 | 0.220 | 3959911.580 |
| 16 | 0.197 | 3775073.000 | 0.197 | 3968471.464 |
| 17 | 0.225 | 6142682.000 | 0.228 | 5885885.480 |
| 18 | 0.183 | 6036633.000 | 0.183 | 6065643.044 |

Table 9 Error of training data set

| Case | Error [ (Desired value – Prediction values) / Desired values ] | |
|---|---|---|
| | Nacelle acceleration | Line tension |
| 1 | 0.017 | 0.009 |
| 2 | 0.006 | 0.036 |
| 3 | 0.017 | 0.080 |
| 4 | 0.007 | 0.075 |
| 6 | 0.008 | 0.096 |
| 7 | 0.004 | 0.025 |
| 8 | 0.002 | 0.002 |
| 9 | 0.013 | 0.006 |
| 11 | 0.019 | 0.042 |
| 12 | 0.013 | 0.003 |
| 13 | 0.018 | 0.012 |
| 14 | 0.040 | 0.068 |
| 16 | 0.000 | 0.051 |
| 17 | 0.015 | 0.042 |
| 18 | 0.001 | 0.005 |

$$e_j(n) = d_j(n) - y_j(n) \tag{6}$$

$$E(n) = \frac{1}{2}\sum_{j=1}^{L} e_j^2(n) \tag{7}$$

Table 8 shows the accuracy of the generated response surface.

Table 9 shows the prediction accuracy of the generated response surface for 15 cases in the training sample. The structure of the neural network is appropriate, because all of the error values are below 0.1.

Tables 10 and 11 show the prediction accuracy of the generated response surface and errors for the test data. Analysis of the results in Table 11 shows that there are still prediction errors. However, to determine the performance in a limited time, the NRSM can give reasonable results for the initial design stage.

### 3.5 Optimization

Table 12 and Fig. 9 show the parameters for NSGA-II and the pareto-optimum sets as the final result of the framework. To select the

Table 10 Analysis results for test data set

| Case | Desired values | | Prediction values | |
|---|---|---|---|---|
| | Nacelle Acceleration (g) | Line tension (N) | Nacelle Acceleration (g) | Line tension (N) |
| 5 | 0.206 | 2876034.250 | 0.196 | 2616009.792 |
| 10 | 0.190 | 3817764.750 | 0.189 | 3189522.020 |
| 15 | 0.249 | 3580220.750 | 0.252 | 4002711.000 |

Table 11 Error of test data set

| Case | Error [ (Prediction value – Desired values) / Desired values ] | |
|---|---|---|
| | Nacelle acceleration | Line tension |
| 5 | 0.045 | 0.090 |
| 10 | 0.002 | 0.165 |
| 15 | 0.011 | 0.118 |

Table 12 NSGA-II Parameter

| Parameter | Value |
|---|---|
| Population size | 150 |
| Generation | 500 |
| Crossover | 20% |
| Mutation | 1% |

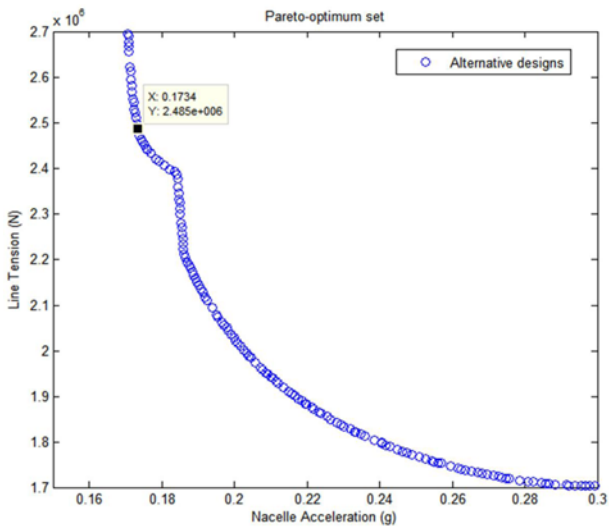


Fig. 9 Pareto-optimum set

final optimum design among the pareto-optimum set, we used a weighting factor. The weighting factors of nacelle acceleration and line tension are 0.6 and 0.5 respectively. The black point is the selected optimum design (Fig. 9). The design variables of the selected design case are S (submerged depth for column, 15 m), H (the height of a cylinder, 28.51 m), and $R_B$ (the cylinder radius, 6.000 m).

### 3.6 Analysis of optimum design

Table 13 shows the performance analysis results of the constructed framework and AQWA result. When using the constructed framework, the prediction error is as high as 0.163 (line tension), as shown in Table 14.

Finally, the improvement in standards of performance evaluation was analysed, as shown in Table 15, where all criteria for the optimum design case decreased against the base design case.

Table 13 Result analysis

| Design variables for optimum design case | | |
|---|---|---|
| S (m) | $R_B$ (m) | H (m) |
| 15.000 | 6.000 | 28.510 |

| NRSM Framework | | AQWA Calculation | |
|---|---|---|---|
| Nacelle acceleration (g) | Line tension (N) | Nacelle acceleration (g) | Line tension (N) |
| 0.173 | 2484726.851 | 0.172 | 2968135.750 |

Table 14 Prediction error

| Prediction error [ (AQWA Calculation – NRSM Framework) / AQWA Calculation ] | |
|---|---|
| Nacelle acceleration | Line tension |
| 0.006 | 0.163 |

Table 15 Improvement for criteria of performance evaluation

| Improvement [ (Base model – Optimization model) / Base model ] | | |
|---|---|---|
| Displacement | Nacelle acceleration | Line tension |
| 0.297 (Decrease) | 0.273 (Decrease) | 0.059 (Decrease) |

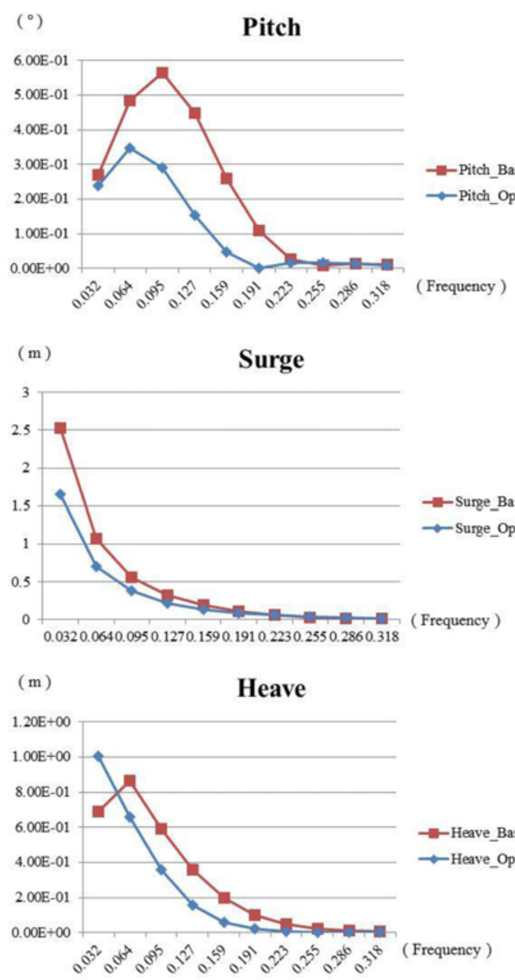


Fig. 10 Performance analysis results

Table 16 Specifications of the final model

| Detail of Model | | |
|---|---|---|
| $R_C$ | 3.000 | m |
| $R_B$ | 6.000 | m |
| H | 28.510 | m |
| S | 15.000 | m |
| Displacement | 3,739,733.045 | kg |
| Tension (Displacement * 0.3) | 1,121,919.914 | kg |
| Pretension | 10,994,815.000 | N |
| Centre of gravity (x, y, z) | (-2, 0, 15.171) | m |

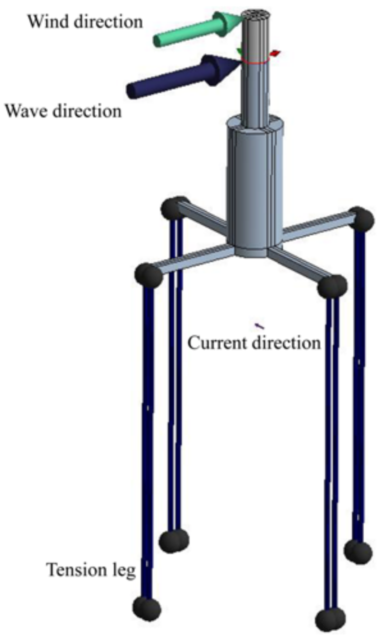


Fig. 11 Optimal sub-structure of TLP type wind-turbine

Fig. 10 shows the hydrodynamic performance of the optimization design case (blue line) in comparison with the base design case (red line) in the frequency domain. The optimization design case motions of pitch, heave, and surge are lower than in the base design case.

Table 16 shows the specifications for the final model. Fig. 11 shows the geometry of the optimization model case.

## 4. Conclusion

The following conclusions were obtained in this study:

I. We proposed the optimization framework based on NRSM:
- The method generates the response surface using BPN.
- The response surface generation procedure is considered as NRSM.
- The system is optimized using NSGA-II.

II. To confirm the prediction accuracy, a non-linear mathematical function was used for a comparison of the response surfaces generated by RSM and NRSM.

III. Through a case study on 5MW TLP-type wind-turbine considering hydrodynamic performance, we confirmed the applicability of the proposed framework for an NAOE optimization problem.

The constructed framework will be improved regarded to the design variable analysis process, and the optimum framework will be applied to various shape optimization problems for naval architecture and ocean engineering.

## ACKNOWLEDGEMENT

This work was supported by the National Research Foundation of Korea (NRF) grant funded by the Korea government (MEST) through GCRC-SOP (No. 2011-0030671).

## REFERENCES

1. Ko, D. H., Ko, D. C., Lim, H. J., Lee, J. M., and Kim, B. M., “Fe-Simulation Coupled with CFD Analysis for Prediction of Residual Stresses Relieved by Cryogenic Heat Treatment of Al6061 Tube,” Int. J. Precis. Eng. Manuf., Vol. 14, No. 8, pp. 1301-1309, 2013.

2. Jung, S. P., Kim, Y. G., and Park, T. W., “A Study on Thermal Characteristic Analysis and Shape Optimization of a Ventilated Disc,” Int. J. Precis. Eng. Manuf., Vol. 13, No. 1, pp. 57-63, 2012.

3. Hong, K. J., Jeon, K. K., Cho, Y. S., Choi, D., and Lee, S. J., “A Study on the Construction of Response Surfaces for Design Optimization,” Transactions of Korean Society of Mechanical Engineering A, Vol. 24, No. 2, pp. 1408-1418, 2000.

4. Myers, R. H., Montgomery, D. C., and Anderson-Cook, C. M., “Response Surface Methodology: Process and Product Optimization Using Designed Experiments,” John Wiley & Sons, 1st Ed., pp. 281-416, 1996.

5. Li, Z. Z., Cheng, T. H., Xuan, D. J., Ren, M., Shen, G. Y., et al., “Optimal Design for Cooling System of Batteries using DOE and RSM,” Int. J. Precis. Eng. Manuf., Vol. 13, No. 9, pp. 1641-1645, 2012.

6. Sarýkaya, M. and Güllü, A., “Taguchi Design and Response Surface Methodology based Analysis of Machining Parameters in CNC Turning under MQL,” Journal of Cleaner Production, Vol. 65, pp. 604-616, 2014.

7. Salman, J. M., “Optimization of Preparation Conditions for Activated Carbon from Palm Oil Fronds using Response Surface Methodology on Removal of Pesticides from Aqueous Solution,” Arabian Journal of Chemistry, Vol. 7, No. 1, pp. 101-108, 2014.

8. Kahraman, F., “The Use of Response Surface Methodology for Prediction and Analysis of Surface Roughness of AISI 4140 Steel,” Materials and Technology, Vol. 43, No. 5, pp. 267-270, 2009.

9. Shin, S. C., “A Study on Prediction of Wake Distribution by Neuro-Fuzzy System,” Journal of Fuzzy Logic and Intelligent Systems, Vol. 17, No. 2, pp. 154-159, 2007.

10. Jian-Hao, X., “Application of Artificial Neural Network (ANN) for

Prediction of Maritime Safety," Information and Management Engineering Communications in Computer and Information Science, Vol. 236, pp. 34-38, 2011.

11. Lee, J. C., Jeong J. H., and Shin, S. C., "A Study on Prediction Method for Added Resistance in Waves using the Genetic Programming," Proc. of the Society of Naval Architects of Korea Annual Autumn Conference, pp.482-490 , 2014.

12. Lee, Y. S. and Choi, Y. B., "Hull Form Optimization based on from Parameter Design," Journal of the Society of Naval Architects of Korea, Vol. 46, No. 6, pp. 562-568, 2009.

13. Kim, H. J., Chun, H. H., and Choi, H. J., "Development of CFD based Stern Form Optimization Method," Journal of the Society of Naval Architects of Korea, Vol. 44, No. 6, pp. 564-571, 2007.

14. Ross, P. J., "Taguchi Techniques for Quality Engineering," McGraw-Hill, 2nd Ed, pp. 43-73, 267-282, 1995.

15. Hecht-Nielsen, R., "Theory of the Backpropagation Neural Network," Proc. of International Joint Conference on Neural Networks, pp. 593-605, 1989.

16. Deb, K., Pratap, A., Agarwal, S., and Meyarivan, T., "A Fast and Elitist Multiobjective Genetic Algorithm: NSGA-II," IEEE Transactions on Evolutionary Computation, Vol. 6, No. 2, pp. 182-197, 2002.

17. Chester, M., "Neural Networks: A Tutorial," Prentice Hall, pp. 50-65, 1993.